

Review

Synergistic Water-Treatment Reactors Using a TiO₂-Modified Ti-Mesh Filter

Tsuyoshi Ochiai^{1,2,*}, Ken Masuko^{2,3}, Shoko Tago¹, Ryuichi Nakano⁴, Kazuya Nakata², Masayuki Hara¹, Yasuhiro Nojima⁵, Tomonori Suzuki^{2,3}, Masahiko Ikekita^{2,3}, Yuko Morito^{2,6}, and Akira Fujishima^{1,2}

¹ Kanagawa Academy of Science and Technology, KSP East 407, 3-2-1 Sakado, Takatsu-ku, Kawasaki, Kanagawa 213-0012, Japan; E-Mails: pg-tago@newkast.or.jp (S.T.); pg-hara@newkast.or.jp (M.H.)

² Photocatalysis International Research Center, Tokyo University of Science, 2641 Yamazaki, Noda, Chiba 278-8510, Japan; E-Mails: nakata@rs.tus.ac.jp (K.N.); fujishima_akira@admin.tus.ac.jp (A.F.)

³ Department of Applied Biological Science, Tokyo University of Science, Yamazaki 2641, Noda, Chiba 278-8510, Japan; E-Mails: j6412647@ed.tus.ac.jp (K.M.); chijun@rs.noda.tus.ac.jp (T.S.); masalab@rs.noda.tus.ac.jp (M.I.)

⁴ Department of Microbiology and Immunology, Teikyo University School of Medicine, 2-11-1 Kaga, Itabashi-ku, Tokyo 173-8605, Japan; E-Mail: nakano@med.teikyo-u.ac.jp

⁵ Kitasato Research Center for Environmental Science, 1-15-1, Kitasato, Minami-ku, Sagami-hara, Kanagawa 252-0329, Japan; E-Mail: nojima@kitasato-e.or.jp

⁶ U-VIX Corporation, 2-14-8 Midorigaoka, Meguro-ku, Tokyo 152-0034, Japan; E-Mail: y.morito@u-vix.com

* Author to whom correspondence should be addressed; E-Mail: pg-ochiai@newkast.or.jp; Tel.: +81-44-819-2040; Fax: +81-44-819-2070.

Received: 26 April 2013; in revised form: 5 June 2013 / Accepted: 11 July 2013 /

Published: 22 July 2013

Abstract: The recent applications of a TiO₂-modified Ti-mesh filter (TMiP™) for water purification are summarized with newly collected data including biological assays as well as sewage water treatment. The water purification reactors consist of the combination of a TMiP, a UV lamp, an excimer VUV lamp, and an ozonation unit. The water purification abilities of the reactor were evaluated by decomposition of organic contaminants, inactivation of waterborne pathogens, and treatment efficiency for sewage water. The UV-C/TMiP/O₃ reactor disinfected *E. coli* in aqueous suspension in approximately 1 min completely, and also decreased the number of *E. coli* in sewage water in 15 min

dramatically. The observed rate constants of 7.5 L/min and 1.3 L/min were calculated by pseudo-first-order kinetic analysis respectively. Although organic substances in sewage water were supposed to prevent the UV-C/TMiP/O₃ reactor from purifying water, the reactor reduced *E. coli* in sewage water continuously. On the other hand, although much higher efficiencies for decomposition of organic pollutants in water were achieved in the excimer/TMiP reactor, the disinfection activity of the reactor for waterborne pathogens was not as effective as the other reactors. The difference of efficiency between organic pollutants and waterborne pathogens in the excimer/TMiP reactor may be due to the size, the structure, and the decomposition mechanism of the organic pollutants and waterborne pathogens. These results show that a suitable system assisted by synergy of photocatalysts and other technologies such as ozonation has a huge potential as a practical wastewater purification system.

Keywords: photocatalysis; TiO₂-modified Ti-mesh filter; ozonation; excimer lamp; advanced oxidation processes; sewage water treatment

1. Introduction

Photocatalytic environmental purification, especially wastewater treatment, has received intensive consideration on cost and enduring stability [1–4]. However, popularly used photocatalyst and photocatalytic filters significantly limit its application because of relatively low purification efficiency [5,6] and difficulty in handling the powder [7–9]. Thus, although many researchers have been working on photocatalytic water purification, it could not be developed to the stage of effective real industrial technology because of the difficulty in fabricating a practical water purifier. Recently we have developed an easy-to-handle photocatalytic filter material, TiO₂ nanoparticles modified titanium mesh (Titanium mesh impregnated photocatalyst, TMiP™), and its applications for environmental purification [4,10–16]. Due to the highly-ordered three-dimensional structure modified with TiO₂ nanoparticles, TMiP provides excellent breathability for both air and water while maintaining a high level of surface contact. Its high flexibility and mechanical stability allow the design of any shape for the unit and for use in relatively severe situations such as inner plasma [11,15]. Based on these results, we summarize in this paper the applications of TMiP for water purification with newly collected data including biological assay and sewage water treatment. The purification abilities of the reactors were evaluated by decomposition of organic contaminants, inactivation of waterborne pathogens, and treatment of sewage water.

2. Materials and Methods

2.1. General Methods

In our experiments, all the reagents were analytical grade and used without further purification. All solutions were made from Milli-Q ultrapure water. The irradiation was provided by the 10 W BLB lamp (FL10BLB, Toshiba, λ_{\max} = 365 nm) or the 18 W UV-C lamp (ZW18D15Y-Z356, Cnlight,

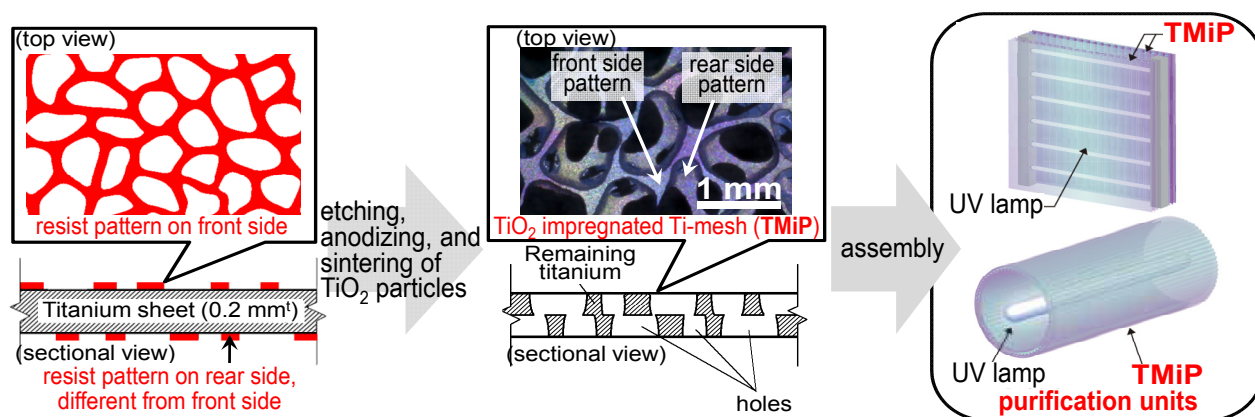
$\lambda_{\max} = 254$ nm). UV intensity was measured with UV power meter C9536/H9535-254 for 254 nm (Hamamatsu Photonics, Hamamatsu, Japan), UV power meter C9536-01/H9958 for 310–380 nm (Hamamatsu Photonics), and UV RADIO METER UV-M03A with UV-SN31 sensor head (ORC Manufacturing, Tokyo, Japan). An ozone gas stream was generated from oxygen gas with a concentration of 0.5 to 10 mg/L by a corona-discharge ozone generator (ED-OG-API, Ecodesign Inc., Tokyo, Japan). The concentration of dissolved O_3 was measured with a Digital pack test for O_3 (Kyoritsu Chemical-Check. Lab., Corp, Tokyo, Japan). The initial concentration of dissolved methylene blue (MB) was controlled to 40 μ M and the MB concentration as a function of treatment time was measured with a UV–visible spectrophotometer at 660 nm (UV-2450, Shimadzu, Kyoto, Japan). The concentration of phenol was measured by HPLC using the previously reported method [17]. Suspended solids (SS) and PtCo Color of sewage water samples were measured by spectrophotometer (DR5000, HACH Company, Loveland, CO, USA). All experiments were carried out at room temperature and atmospheric pressure.

Escherichia coli NBRC13965 (*E. coli*), *Legionella pneumophila* ATCC49249 (*L. pneumophila*), Q β phage NBRC20012 (Q β), and *feline calicivirus* F-9 ATCC VR-782 (FCV) were used as the main test waterborne pathogens to assess the biological purification efficiency of the units. *E. coli* and Q β were obtained from the Biological Resource Center of the National Institute of Technology and Evaluation (Chiba, Japan). *L. pneumophila* and FCV were obtained from American Type Culture Collection (Manassas, VA, USA). *E. coli*, *L. pneumophila*, and Q β were propagated and assayed by previously described methods [14,18–20]. FCV was propagated and assayed by the plaque technique on confluent layers of Crandell-Reese feline kidney cell cultures grown in 12-well culture plates as described elsewhere [21]. Standard Plate Count (SPC), Total Coliform (TC), and *E. coli* in sewage water sample were also assayed by previously described methods [17]. The SPC is usually reported as the number of all of the bacteria per milliliter of sample. There are no drinking water standards for SPC, but if more than 500 bacteria are counted in one milliliter of sample, further testing for TC or *E.coli* is suggested. The TC is reported as the number of a whole group of the coliform bacteria which can cause and indicate potential health problems. *E. coli* is considered to be the major species of coliform bacteria that is the best indicator of fecal pollution and the possible presence of pathogens.

2.2. Fabrication of TMiP

The detailed preparation procedure and characterization of TMiP were described in a previous report [10]. The procedure is briefly shown in Figure 1. The Ti-mesh, obtained by controlled chemical etching of 0.2 mm^t titanium foil, was anodized at a voltage of 70 V to give a violet color in acid solution. The resulting structure was controlled by mask pattern and etching time as shown in Figure 1 and the colors were able to be controlled by anodizing voltage and time [13]. Then the Ti-mesh was treated at 550 °C for 3 h to produce a TiO₂ layer on the Ti-mesh surface. The treated Ti-mesh was dip-coated with 25 wt % of TiO₂ anatase sol (TKD-701, TAYCA, Osaka, Japan) and was heated at 550 °C for 3 h. The structural and surface morphology of TMiP were examined and studied by using X-ray diffraction and Scanning Electron Microscopy.

Figure 1. Fabrication method of TiO₂ nanoparticles modified titanium mesh (TMiP™). Reproduced with permission from Ochiai *et al.* [10], Catalysis Science and Technology; published by RSC Publishing, 2011.



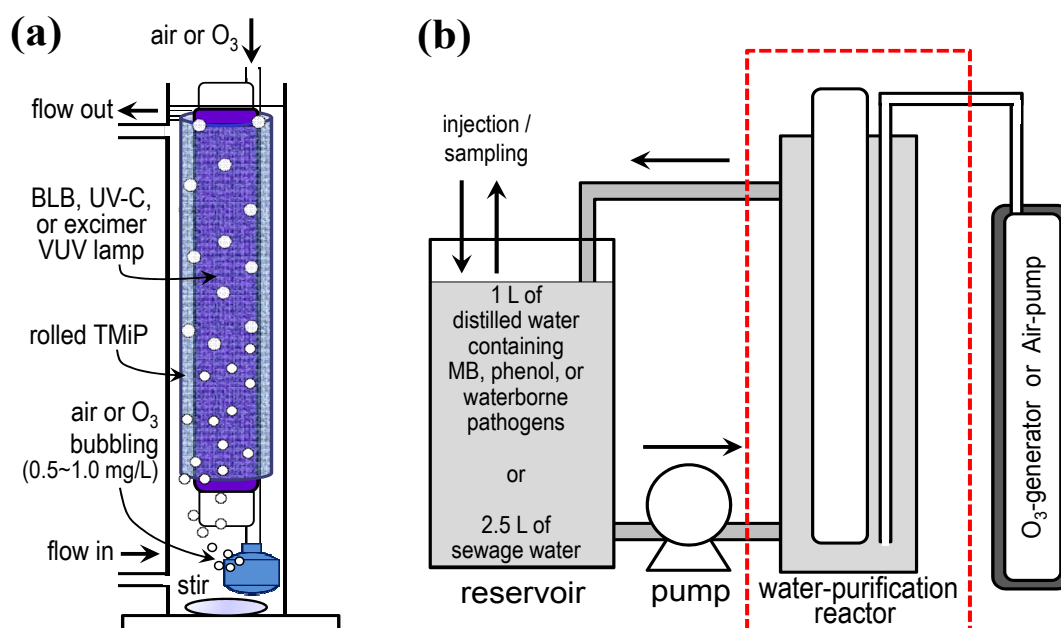
2.3. Fabrication of the Water Purification System Using TMiP

Figure 2a shows schematic illustrations of water-purification reactors. The reactors consist of an acrylic tube (49 mm i.d. × 400 mm length) with two ports, TMiP with UV lamps [BLB lamp (10 W, 6.0 mW cm⁻² at 310–380 nm), UV-C lamp (10 W, 10 mW cm⁻² at 254 nm), or excimer VUV lamp (7.2 mW cm⁻² at 172 nm)], and a bubbling unit (air or ozone). For comparison of the effect of UV wavelength and air or O₃ bubbling, the combinations of the reactors were investigated [e.g., BLB/TMiP, BLB/TMiP/O₃, O₃ bubbling alone, and the excimer lamp unit wrapped with Ti-mesh without TiO₂ nanoparticles (excimer alone unit)]. O₃ dose was varied at 0.5–1.0 mg/L or 10 mg/L. The basic design and fabrication method of the excimer/TMiP reactor were described previously [12,16]. When the alternating current (AC) high voltage is applied to the electrodes, the dielectric barrier discharge occurs in the quartz tube which provides intense narrow band radiation at 172 nm from a xenon excimer (Xe₂^{*}) [22]. UV intensity was measured by UV power meters as mentioned in Section 2.1. Figure 2b shows the schematic illustration of a water purification system which consists of the water-purification reactors shown in Figure 2a, a reservoir, a pump, and an O₃ production unit or an air pump. An aqueous solution containing organic contaminants or waterborne pathogens was circulated through the tube by the pump and was treated in the reactor.

2.4. Test Method for Evaluation of the Water Purification Ability of the System

Water purification ability of the units was evaluated by tests of MB decolorization, phenol decomposition, and inactivation of waterborne pathogens. In a typical run, one liter of an aqueous solution containing 40 μM MB was circulated through the reactor by the pump at a flow rate of 100 mL/min. The concentration of dissolved MB as a function of treatment time was measured with a UV–visible spectrophotometer. Similarly, 1 L of an aqueous suspension of *E. coli* was used as the biologically contaminated water sample and was circulated through the reactor by the pump at a flow rate of 1 L/min. The viability of waterborne pathogens in the artificially contaminated water samples was analyzed with previously reported methods [14,18–21].

Figure 2. Schematic illustrations of (a) water-purification reactor and (b) water-purification system. Reproduced with permission from Ochiai *et al.* [10,14,16], Catalysis Science and Technology; published by RSC Publishing, 2011.



In this paper, a sewage water purification test was introduced as an experiment for practical use. The sewage water samples were collected from a sewage treatment plant which has a primary unit, two secondary units, and a tertiary treatment unit. The primary treatment unit consists of a mechanical screen, a grit removal tank, and a primary clarifier. The sewage treatment plant has two secondary treatment units in parallel; both units perform anoxic–oxic–anoxic–oxic-based biological nutrient removal. The main difference between them is the source of oxygen in the aeration tank: ambient air in unit I and pure oxygen in unit II. Units I and II are followed by ozonation as the tertiary treatment. To investigate the purification ability of the system for usage as an alternative for the tertiary treatment unit, sewage water samples were collected in 10 L plastic tank from the sewage treatment plant at the inlet of the tertiary treatment unit on 5 September 2011 and 18 July 2012. After addition of *E. coli* suspension to control initial viability of bacteria to approximately 10^6 Colony Forming Unit (CFU)/mL, the sewage water sample (2.5 L) was circulated through the reactor by the pump at a flow rate of 1 L/min. The viability of bacteria in the sewage water samples was analyzed with the above mentioned methods.

3. Results and Discussion

3.1. Water-Purification Ability of the Reactors Evaluated by Methylene Blue Decolorization

Figure 3 shows MB decolorization without any reactors (blank, crosses), by the BLB/TMiP reactor (open triangles), and by the BLB/TMiP/air reactor (solid diamonds). The MB concentrations were well fitted with a pseudo-first-order kinetics given by the following equation: $C = C_0 \exp(-k_1 t)$. Where C_0 is the initial MB concentration and k_1 is the observed rate constant. The values of k_1 were calculated by exponential fitting of Figure 3 to 0.60 and 0.82 h^{-1} for the BLB/TMiP and the BLB/TMiP/air reactors,

respectively. Interestingly, the BLB/TMiP/air reactor showed a higher decolorization rate than the BLB/TMiP reactor. Tasbihi *et al.* reported that dissolved oxygen could improve the efficiency of the degradation of organics by enhancing the separation of photogenerated electron-hole pairs, thereby increasing $\cdot\text{OH}$ concentration [23]. Thus, the excellent accessibility of the TMiP structure enhanced the air bubbling effect and resulted in higher decolorization. Evidence for this is shown in a previous report by comparison with TiO_2 -modified commercial Ti-mesh (200×200 mm, 0.30 mm ϕ , 20 mesh, Nilaco) [10]. Interestingly, the SEM images of TiO_2 -modified commercial Ti-mesh did not show the well dispersed spherical particles of TiO_2 on the surface. This may be caused by the difference between the good morphology of TMiP and the monotonous structure of commercial Ti-mesh. The BLB/TMiP/ O_3 reactor was also evaluated by the MB decolorization test; however, the MB color suddenly disappeared due to extreme oxidation activity of the reactor. The water-purification ability of the BLB/TMiP/ O_3 reactor is discussed in the next paragraph by comparison with the ability of O_3 bubbling alone.

Figure 3. Methylene blue (MB) decolorization by the water-purification reactors. Crosses: blank; open triangles: BLB/TMiP reactor; solid diamonds: BLB/TMiP/air reactor. Reproduced with permission from Ochiai *et al.* [10], Catalysis Science and Technology; published by RSC Publishing, 2011.

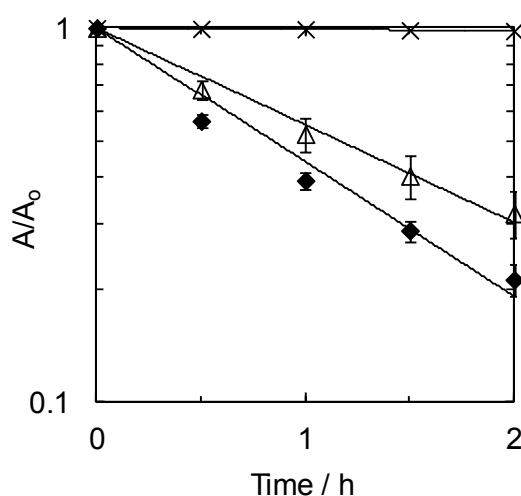
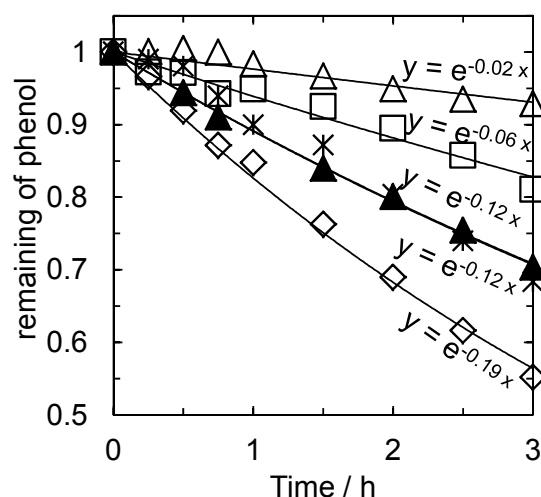


Figure 4 shows the phenol decomposition by BLB/TMiP (open triangles), O_3 bubbling alone (open squares), BLB/TMiP/ O_3 (solid triangles), excimer alone (asterisks), and excimer/TMiP (open diamonds) reactors. The phenol concentrations were also well fitted with a pseudo-first-order kinetics in all reactors. The values of k_1 for the reactors were calculated and are indicated in Figure 4. It can be seen that phenol was effectively decomposed by the BLB/TMiP/ O_3 reactor, compared with O_3 bubbling alone or the BLB/TMiP reactors. Interestingly, although without O_3 bubbling, the excimer/TMiP reactor shows the highest k_1 among reactors. We ascribed the results to reactive species and oxidative intermediates generated by VUV photolysis of water as mentioned by Oppenländer *et al.* [24–28]. Hydroxyl radicals and other reactive species are formed by VUV photolysis of water and can directly react with organics due to their strong oxidation potentials. As a result, the excimer/TMiP reactor is much more efficient than the other reactors.

Figure 4. Phenol decomposition with exponential curve fitting for the water-purification reactors. Open triangles: BLB/TMiP reactor; open squares: O₃ bubbling alone (0.5–1.0 mg/L); solid triangles: BLB/TMiP/O₃ reactor (0.5–1.0 mg/L); asterisks: excimer alone; open diamonds: excimer/TMiP reactor. Reproduced with permission from Ochiai *et al.* [16], Chemical Engineering Journal; published by Elsevier, 2013.

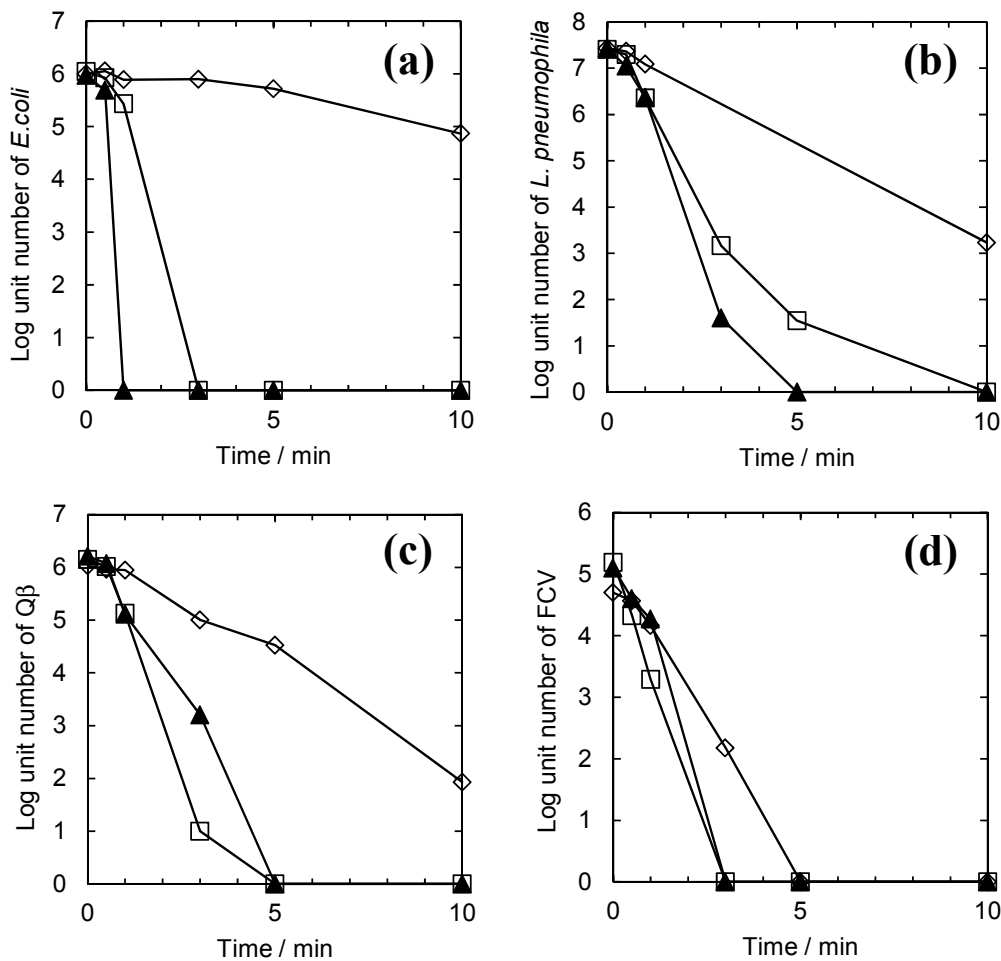


3.2. Water-Purification Ability of the Reactors Evaluated by the Inactivation of Waterborne Pathogens

Figure 5 shows the time courses of the log number of *E. coli* (a), *L. pneumophila* (b), Q β (c), and FCV (d) in the water purification system with the O₃ bubbling alone (open squares), BLB/TMiP/O₃ (solid triangles), and excimer/TMiP (open diamonds) reactors. The disinfection activity of the BLB/TMiP/O₃ reactor is higher than the O₃ alone condition for *E. coli*, and *L. pneumophila*. On the other hand, the activity of the BLB/TMiP/O₃ reactor was not so effective on comparison with the BLB/TMiP reactor for Q β and FCV. Moreover, disinfection activity of the excimer/TMiP was lower than the other reactors especially for *E. coli*. The difference in the activity of the reactors among the waterborne pathogens may be due to the size of molecules or bacteria, the surface composition of bacteria or viruses, the critical wavelength for disinfection, and the permeation ability of reactive species. Oppenländer *et al.* also reported VUV-induced oxidation of organics in homogeneous aqueous solution within a xenon-excimer flow-through photoreactor [24]. They found that the decomposition rate was strongly influenced by the size and the structure of the organics, e.g., the homologous series of saturated alcohols C₁–C₈ was decomposed in descending order of the TOC degraded after an irradiation time of 3 h. In this series 1-octanol was decomposed with the lowest efficiency because of the highest statistical possibility of formation of intermediate products. In addition, the path that 172 nm VUV light penetrates the water is very short due to the high absorption coefficients of water [29,30]. Therefore, no matter what oxidant was produced by VUV photolysis, it would not be consumed by the purification process due to the long distance (several millimeters) [31]. On the other hand, Cho *et al.* reported the difference of efficiency among waterborne pathogens by reactive oxygen species [32–37]. These studies indicate that bacteria could be inactivated by all forms of reactive oxygen species produced by photocatalysis, while viruses demonstrate notably higher resistance to photocatalytic inactivation. Since the structures of Q β and FCV, compared to *E. coli* and *L. pneumophila*, are simpler, Q β and FCV were

susceptible to $\bullet\text{OH}$ and were not very susceptible to less reactive species such as $\text{O}_2^{\bullet-}$. In addition, the germicidal effect of UV-C is critical for disinfection [38,39]. On the contrary, VUV and UV-A are less important for it than the UV-C [40]. Our data clearly show this tendency.

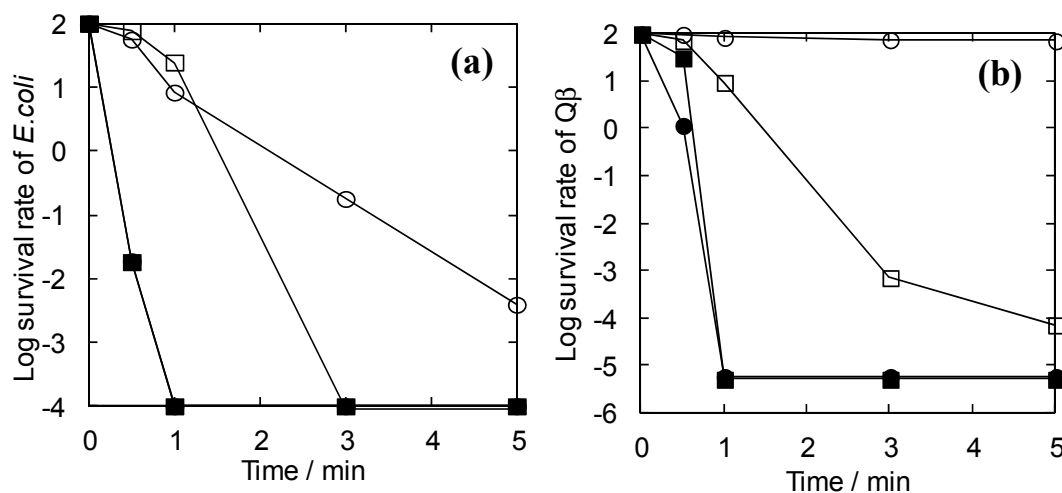
Figure 5. Time courses of log number of (a) *E. coli*; (b) *L. pneumophila*; (c) Q β ; and (d) FCV in the water purification system. Open squares: O₃ bubbling alone (0.5–1.0 mg/L); solid triangles: BLB/TMiP/O₃ reactor (0.5–1.0 mg/L); open diamonds: excimer/TMiP reactor.



3.3. Water-Purification Ability of the Reactors Using the Higher Concentration of O₃ and UV-C

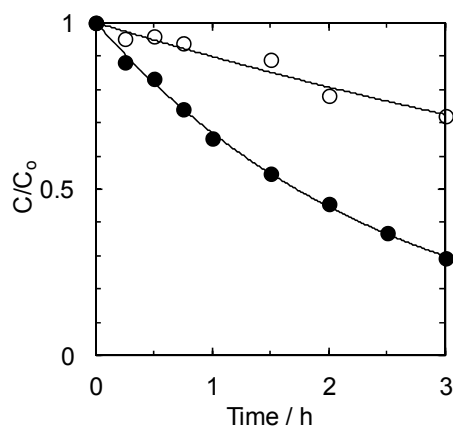
The result of the inactivation test by using the higher concentration of O₃ and UV-C shows the above-mentioned tendency more clearly (Figure 6). By using the UV-C/TMiP reactor, more than 5 min of treatment time is required for total inactivation of *E. coli* (Figure 6a, open circles). In contrast, 0.5–1.0 mg/L of O₃ bubbling (Figure 6a, open squares) takes a shorter treatment time (less than 3 min) for the inactivation and there is no difference between 10 mg/L of O₃ bubbling (Figure 6a, solid squares) and UV-C/TMiP/O₃ (10 mg/L) reactor (Figure 6a, solid circles, overlapped on solid squares). On the other hand, Q β was not inactivated efficiently by the UV-C/TMiP reactor (Figure 6b, open circles) and 0.5–1.0 mg/L of O₃ bubbling (Figure 6b, open squares). However, with 10 mg/L of O₃ bubbling (Figure 6b, solid squares) the UV-C/TMiP/O₃ (10 mg/L) reactor (Figure 6b, solid circles) inactivated Q β efficiently (less than 1 min).

Figure 6. Time course of log survival rate of (a) *E. coli*; and (b) Q β in the water purification system. open circles: UV-C/TMiP reactor; open squares: O₃ alone (0.5–1.0 mg/L); solid squares: O₃ alone (10 mg/L); solid circles: UV-C/TMiP/O₃ reactor (10 mg/L). Reproduced with permission from Ochiai *et al.* [14], Catalysis Science and Technology; published by RSC Publishing, 2011.



Similarly, the time course of phenol concentration in the water purification system with the UV-C/TMiP/O₃ (10 mg/L) reactor (Figure 7, solid circles) is larger than with the UV-C/TMiP reactor (Figure 7, open circles). This result indicates that the UV-C/TMiP/O₃ reactor was able to decompose phenol more efficiently than the UV-C/TMiP reactor. Here O₃ is a good acceptor of excited electrons the same as O₂. Thus, •OH production and photocatalytic oxidation are enhanced by the presence of O₃, which prevents carrier recombination in photocatalysis [41–44]. Moreover, O₃⁻ can oxidize organics with a relatively long lifetime [45,46]. On the other hand, there are many reports about photolytic/catalytic decomposition of O₃ [47–50]. Highly oxidative intermediates such as atomic oxygen could be produced from O₃ by UV-C irradiation and/or the presence of heterogeneous catalyst surfaces. In this case, UV-C irradiation and the large specific surface area of TMiP could decompose O₃ effectively [11].

Figure 7. Phenol decomposition by the water-purification system. open circles: UV-C/TMiP reactor; solid circles: UV-C/TMiP/O₃ reactor (10 mg/L). Reproduced with permission from Ochiai *et al.* [16], Chemical Engineering Journal; published by Elsevier, 2013.



3.4. Treatment of Sewage Water Samples

Figure 8 shows the time course of SS and PtCo Color of the sewage water samples in the water-purification systems. There was almost no difference between the UV-C/TMiP/O₃ reactor (10 mg/L, solid circles) and the O₃ bubbling alone condition (10 mg/L, solid squares) for reduction of both SS (Figure 8a) and PtCo Color (Figure 8b). It is known that these factors ultimately decrease the photocatalytic efficiency of water treatment [3,51,52]. On the other hand, adding ozone to the water purification system results in an overall improvement in water quality due to more complete oxidation of color, organics, and suspended solids [53,54]. At the same time, ozone-induced microflocculation can reduce SS [55]. The present data well support these phenomena. However, interestingly, the time courses of survival rate of SPC (Figure 9a), TC (Figure 9b), and *E. coli* (Figure 9c) in the water purification systems show that the disinfection activity of the UV-C/TMiP/O₃ reactor is higher than the O₃ bubbling alone condition. These results were also ascribed to the synergistic effect of photocatalysis and ozonation as mentioned in Section 3.3. In addition, the germicidal effect of UV-C with the formation of pyrimidine dimers in the DNA is critical for disinfection [38,39]. On the contrary, VUV and UV-A are less important for sterilization than the UV-C [40]. Our data clearly show this tendency. However, the calculated rate constant, k_1 , for pseudo-first-order kinetics of *E. coli* disinfection was 1.3 L/min (normalized by sample volume) in the treatment of a sewage water sample. This value is approximately 18% of the value for the kinetics of *E. coli* disinfection in aqueous suspension (7.5 L/min, calculated from Figure 6a). This result suggests that refractory organic substances such as humic substances or SS may affect the rate of disinfection [51,52].

Figure 8. Time course of (a) SS and (b) PtCo Color of the sewage water in the water-purification system. solid squares: O₃ bubbling (10 mg/L); solid circles: UV-C/TMiP/O₃ reactor (10 mg/L).

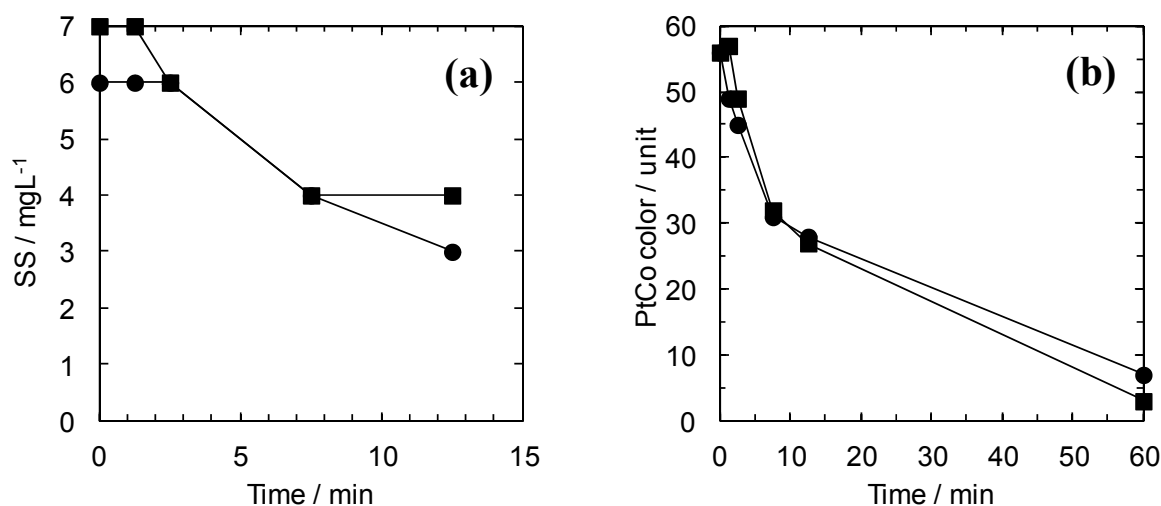
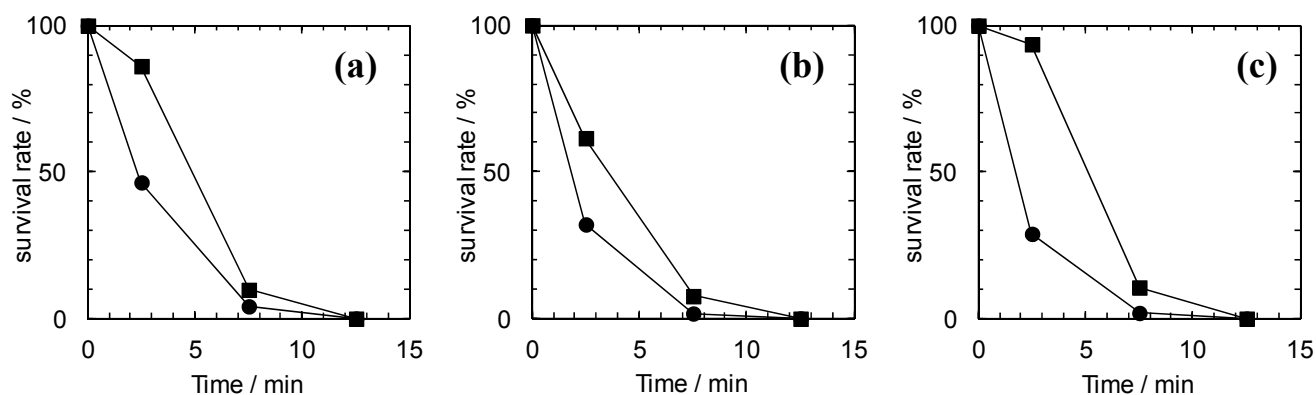


Figure 9. Time course of survival rate of (a) SPC; (b) TC; and (c) *E. coli* in the water purification system. Solid squares: O₃ bubbling (10 mg/L); solid circles: UV-C/TMiP/O₃ reactor (10 mg/L).



4. Conclusions

The high efficiency for decomposition of chemical and biological contaminants results from the highly-ordered three dimensional structure of TMiP and the synergistic effect of photocatalysis and other technologies such as ozonation or excimer VUV lamp. The excimer-lamp-assisted photocatalysis (excimer/TMiP unit) achieved high efficiency for decomposition of dissolved phenol in water compared with the photolysis (excimer alone unit), ozonation (O₃ alone unit), photocatalysis (BLB/TMiP and UV-C/TMiP units), and ozone-assisted photocatalysis (BLB/TMiP + O₃ unit). On the other hand, the disinfection activity of the excimer/TMiP unit for waterborne pathogens was not so effective compared with the other units. The reaction mechanism in this research can be formulated as follows. Photochemically generated •OH which is the dominant reactive species in the excimer/TMiP unit could decompose phenol and viruses efficiently. On the contrary, because of the difference of the size and the decomposition mechanism, it may be difficult to decompose the bacterial cell wall by an excimer/TMiP unit compared with phenol and viruses. Ozone could attack the cell wall and the surface components of bacteria and then disrupt its integrity by its extremely strong oxidation potential. Therefore, O₃ alone and BLB/TMiP + O₃ units could inactivate bacteria efficiently compared with an excimer/TMiP unit.

Acknowledgments

The work was supported in part by the Kurata Memorial Hitachi Science and Technology Foundation. The authors are grateful to Hayato Nanba, Toru Hoshi, Yoshihiro Koide (Kanagawa University), Touko Nakagawa (Tokyo University of Science), Etsuko T. Utagawa (National Institute of Infectious Diseases), Yasuji Niitsu, Go Kobayashi, Masahiro Kurano, Izumi Serizawa (ORC Manufacturing Co., Ltd.), Koji Horio, Koji Mori, and Hiro Tatejima (U-VIX Corporation) for the experiments, the helpful advice and discussions, and the supervisions.

Conflict of Interest

The authors declare no conflict of interest.

References

1. Fujishima, A.; Honda, K. Electrochemical photolysis of water at a semiconductor electrode. *Nature* **1972**, *238*, 37–38.
2. Fujishima, A.; Zhang, X.; Tryk, D.A. TiO₂ photocatalysis and related surface phenomena. *Surf. Sci. Rep.* **2008**, *63*, 515–582.
3. Chong, M.N.; Jin, B.; Chow, C.W.K.; Saint, C. Recent developments in photocatalytic water treatment technology: A review. *Water Res.* **2010**, *44*, 2997–3027.
4. Ochiai, T.; Fujishima, A. Photoelectrochemical properties of TiO₂ photocatalyst and its applications for environmental purification. *J. Photochem. Photobiol. C* **2012**, *13*, 247–262.
5. Ollis, D.F. Photocatalytic purification and remediation of contaminated air and water. *C. R. Acad. Sci. II C* **2000**, *3*, 405–411.
6. Ollis, D.F.; Pelizzetti, E.; Serpone, N. Photocatalyzed destruction of water contaminants. *Environ. Sci. Technol.* **1991**, *25*, 1522–1529.
7. Prieto-Rodriguez, L.; Miralles-Cuevas, S.; Oller, I.; Agüera, A.; Puma, G.L.; Malato, S. Treatment of emerging contaminants in wastewater treatment plants (WWTP) effluents by solar photocatalysis using low TiO₂ concentrations. *J. Hazard. Mater.* **2012**, *211–212*, 131–137.
8. Chen, M.; Chu, W. Degradation of antibiotic norfloxacin in aqueous solution by visible-light-mediated C-TiO₂ photocatalysis. *J. Hazard. Mater.* **2012**, *219–220*, 183–189.
9. Sánchez, L.; Peral, J.; Domènech, X. Aniline degradation by combined photocatalysis and ozonation. *Appl. Catal. B Environ.* **1998**, *19*, 59–65.
10. Ochiai, T.; Hoshi, T.; Slimen, H.; Nakata, K.; Murakami, T.; Tatejima, H.; Koide, Y.; Houas, A.; Horie, T.; Morito, Y.; *et al.* Fabrication of TiO₂ nanoparticles impregnated titanium mesh filter and its application for environmental purification unit. *Catal. Sci. Technol.* **2011**, *1*, 1324–1327.
11. Ochiai, T.; Nakata, K.; Murakami, T.; Morito, Y.; Hosokawa, S.; Fujishima, A. Development of an air-purification unit using a photocatalysis-plasma hybrid reactor. *Electrochemistry* **2011**, *79*, 838–841.
12. Ochiai, T.; Niitsu, Y.; Kobayashi, G.; Kurano, M.; Serizawa, I.; Horio, K.; Nakata, K.; Murakami, T.; Morito, Y.; Fujishima, A. Compact and effective photocatalytic air-purification unit by using of mercury-free excimer lamps with TiO₂ coated titanium mesh filter. *Catal. Sci. Technol.* **2011**, *1*, 1328–1330.
13. Ochiai, T.; Nakata, K.; Murakami, T.; Horie, T.; Morito, Y.; Fujishima, A. Anodizing effects of titanium-mesh surface for fabrication of photocatalytic air purification filter. *Nanosci. Nanotechnol. Lett.* **2012**, *4*, 544–547.
14. Ochiai, T.; Nanba, H.; Nakagawa, T.; Masuko, K.; Nakata, K.; Murakami, T.; Nakano, R.; Hara, M.; Koide, Y.; Suzuki, T.; *et al.* Development of an O₃-assisted photocatalytic water-purification unit by using a TiO₂ modified titanium mesh filter. *Catal. Sci. Technol.* **2012**, *2*, 76–78.
15. Ochiai, T.; Hayashi, Y.; Ito, M.; Nakata, K.; Murakami, T.; Morito, Y.; Fujishima, A. An effective method for a separation of smoking area by using novel photocatalysis-plasma synergistic air-cleaner. *Chem. Eng. J.* **2012**, *209*, 313–317.

16. Ochiai, T.; Masuko, K.; Tago, S.; Nakano, R.; Niitsu, Y.; Kobayashi, G.; Horio, K.; Nakata, K.; Murakami, T.; Hara, M.; *et al.* Development of a hybrid environmental purification unit by using of excimer VUV lamps with TiO₂ coated titanium mesh filter. *Chem. Eng. J.* **2013**, *218*, 327–332.
17. Ochiai, T.; Nakata, K.; Murakami, T.; Fujishima, A.; Yao, Y.Y.; Tryk, D.A.; Kubota, Y. Development of solar-driven electrochemical and photocatalytic water treatment system using a boron-doped diamond electrode and TiO₂ photocatalyst. *Water Res.* **2010**, *44*, 904–910.
18. Yao, Y.; Ochiai, T.; Ishiguro, H.; Nakano, R.; Kubota, Y. Antibacterial performance of a novel photocatalytic-coated cordierite foam for use in air cleaners. *Appl. Catal. B Environ.* **2011**, *106*, 592–599.
19. Yao, Y.; Kubota, Y.; Murakami, T.; Ochiai, T.; Ishiguro, H.; Nakata, K.; Fujishima, A. Electrochemical inactivation kinetics of boron-doped diamond electrode on waterborne pathogens. *J. Water Health* **2011**, *9*, 534–543.
20. Yamauchi, K.; Yao, Y.; Ochiai, T.; Sakai, M.; Kubota, Y.; Yamauchi, G. Antibacterial activity of hydrophobic composite materials containing a visible-light-sensitive photocatalyst. *J. Nanotechnol.* **2011**, *2011*, doi: 10.1155/2011/380979.
21. Kreuzt, L.C.; Seal, B.S.; Mengeling, W.L. Early interaction of feline calicivirus with cells in culture. *Arch. Virol.* **1994**, *136*, 19–34.
22. Nohr, R.S.; MacDonald, J.G.; Kogelschatz, U.; Mark, G.; Schuchmann, H.P.; von Sonntag, C. Application of excimer incoherent-UV sources as a new tool in photochemistry: photodegradation of chlorinated dibenzodioxins in solution and adsorbed on aqueous pulp sludge. *J. Photochem. Photobiol. A* **1994**, *79*, 141–149.
23. Tasbihi, M.; Ngah, C.R.; Aziz, N.; Mansor, A.; Abdullah, A.Z.; Teong, L.K.; Mohamed, A.R. Lifetime and regeneration studies of various supported TiO₂ photocatalysts for the degradation of phenol under UV-C light in a batch reactor. *Ind. Eng. Chem. Res.* **2007**, *46*, 9006–9014.
24. Oppenländer, T.; Gliese, S. Mineralization of organic micropollutants (homologous alcohols and phenols) in water by vacuum-UV-oxidation (H₂O-VUV) with an incoherent xenon-excimer lamp at 172 nm. *Chemosphere* **2000**, *40*, 15–21.
25. Oppenländer, T.; Walddörfer, C.; Burgbacher, J.; Kiermeier, M.; Lachner, K.; Weinschrott, H. Improved vacuum-UV (VUV)-initiated photomineralization of organic compounds in water with a xenon excimer flow-through photoreactor (Xe* lamp, 172 nm) containing an axially centered ceramic oxygenator. *Chemosphere* **2005**, *60*, 302–309.
26. Oppenländer, T. Mercury-free sources of VUV/UV radiation: Application of modern excimer lamps (excilamps) for water and air treatment. *J. Environ. Eng. Sci.* **2007**, *6*, 253–264.
27. Afzal, A.; Oppenländer, T.; Bolton, J.R.; El-Din, M.G. Anatoxin—A degradation by advanced oxidation processes: Vacuum-UV at 172 nm, photolysis using medium pressure UV and UV/H₂. *Water Res.* **2010**, *44*, 278–286.
28. Wang, D.; Oppenländer, T.; El-Din, M.G.; Bolton, J.R. Comparison of the disinfection effects of Vacuum-UV (VUV) and UV light on *Bacillus subtilis* spores in aqueous suspensions at 172, 222 and 254 nm. *Photochem. Photobiol.* **2010**, *86*, 176–181.
29. Heit, G.; Neuner, A.; Saugy, P.-Y.; Braun, A.M. Vacuum-UV (172 nm) actinometry. The quantum yield of the photolysis of water. *J. Phys. Chem. A* **1998**, *102*, 5551–5561.

30. Weeks, J.L.; Meaburn, G.M.A.C.; Gordon, S. Absorption coefficients of liquid water and aqueous solutions in the far ultraviolet. *Radiat. Res.* **1963**, *19*, 559–567.
31. Han, W.; Zhang, P.; Zhu, W.; Yin, J.; Li, L. Photocatalysis of p-chlorobenzoic acid in aqueous solution under irradiation of 254 nm and 185 nm UV light. *Water Res.* **2004**, *38*, 4197–4203.
32. Cho, M.; Chung, H.; Yoon, J. Disinfection of water containing natural organic matter by using ozone-initiated radical reactions. *Appl. Environ. Microbiol.* **2003**, *69*, 2284–2291.
33. Cho, M.; Chung, H.; Choi, W.; Yoon, J. Linear correlation between inactivation of *E. coli* and OH radical concentration in TiO₂ photocatalytic disinfection. *Water Res.* **2004**, *38*, 1069–1077.
34. Cho, M.; Chung, H.; Choi, W.; Yoon, J. Different inactivation behaviors of MS-2 phage and *Escherichia coli* in TiO₂ photocatalytic disinfection. *Appl. Environ. Microbiol.* **2005**, *71*, 270–275.
35. Cho, M.; Yoon, J. Measurement of OH radical CT for inactivating cryptosporidium parvum using photo/ferrioxalate and photo/TiO₂ systems. *J. Appl. Microbiol.* **2008**, *104*, 759–766.
36. Cho, M.; Gandhi, V.; Hwang, T.M.; Lee, S.; Kim, J.H. Investigating synergism during sequential inactivation of MS-2 phage and *Bacillus subtilis* spores with UV/H₂O₂ followed by free chlorine. *Water Res.* **2011**, *45*, 1063–1070.
37. Cho, M.; Cates, E.L.; Kim, J.H. Inactivation and surface interactions of MS-2 bacteriophage in a TiO₂ photoelectrocatalytic reactor. *Water Res.* **2011**, *45*, 2104–2110.
38. Chatzisymeon, E.; Droumpali, A.; Mantzavinos, D.; Venieri, D. Disinfection of water and wastewater by UV-A and UV-C irradiation: Application of real-time PCR method. *Photochem. Photobiol. Sci.* **2011**, *10*, 389–395.
39. Oguma, K.; Katayama, H.; Ohgaki, S. Photoreactivation of legionella pneumophila after inactivation by low- or medium-pressure ultraviolet lamp. *Water Res.* **2004**, *38*, 2757–2763.
40. Halfmann, H.; Denis, B.; Bibinov, N.; Wunderlich, J.; Awakowicz, P. Identification of the most efficient VUV/UV radiation for plasma based inactivation of *Bacillus atrophaeus* spores. *J. Phys. D* **2007**, *40*, doi:10.1088/0022-3727/40/19/019.
41. Beltrán, F.J.; Rivas, F.J.; Gimeno, O.; Carbajo, M. Photocatalytic enhanced oxidation of fluorene in water with ozone. Comparison with other chemical oxidation methods. *Ind. Eng. Chem. Res.* **2005**, *44*, 3419–3425.
42. Nishimoto, S.; Mano, T.; Kameshima, Y.; Miyake, M. Photocatalytic water treatment over WO₃ under visible light irradiation combined with ozonation. *Chem. Phys. Lett.* **2010**, *500*, 86–89.
43. Nicolas, M.; Ndour, M.; Ka, O.; D'Anna, B.; George, C. Photochemistry of atmospheric dust: Ozone decomposition on illuminated titanium dioxide. *Environ. Sci. Technol.* **2009**, *43*, 7437–7442.
44. Rivas, F.J.; Beltrán, F.J.; Gimeno, O.; Carbajo, M. Fluorene oxidation by coupling of ozone, radiation, and semiconductors: A mathematical approach to the kinetics. *Ind. Eng. Chem. Res.* **2006**, *45*, 166–174.
45. Nakamura, R.; Sato, S. Oxygen species active for photooxidation of n-decane over TiO₂ Surfaces. *J. Phys. Chem. B* **2002**, *106*, 5893–5896.
46. Einaga, H.; Ogata, A.; Futamura, S.; Ibusuki, T. The stabilization of active oxygen species by Pt supported on TiO₂. *Chem. Phys. Lett.* **2001**, *338*, 303–307.
47. Huang, H.B.; Ye, D.Q.; Leung, D.Y.C. Removal of toluene using UV-irradiated and nonthermal plasma-driven photocatalyst system. *J. Environ. Eng.* **2010**, *136*, 1231–1236.

48. Einaga, H.; Futamura, S. Catalytic oxidation of benzene with ozone over alumina-supported manganese oxides. *J. Catal.* **2004**, *227*, 304–312.
49. Song, S.; Liu, Z.; He, Z.; Zhang, A.; Chen, J.; Yang, Y.; Xu, X. Impacts of morphology and crystallite phases of titanium oxide on the catalytic ozonation of phenol. *Environ. Sci. Technol.* **2010**, *44*, 3913–3918.
50. Guillard, C. Photocatalytic degradation of butanoic acid: Influence of its ionisation state on the degradation pathway: Comparison with O₃/UV process. *J. Photochem. Photobiol. A* **2000**, *135*, 65–75.
51. Phillips, S.L.; Olesik, S.V. Initial characterization of humic acids using liquid chromatography at the critical condition followed by size-exclusion chromatography and electrospray ionization mass spectrometry. *Anal. Chem.* **2003**, *75*, 5544–5553.
52. Jiang, J.; Kappler, A. Kinetics of microbial and chemical reduction of humic substances: Implications for electron shuttling. *Environ. Sci. Technol.* **2008**, *42*, 3563–3569.
53. Navarro, P.; Sarasa, J.; Sierra, D.; Esteban, S.; Ovelleiro, J.L. Degradation of wine industry wastewaters by photocatalytic advanced oxidation. *Water Sci. Technol.* **2005**, *51*, 113–120.
54. Miguel, N.; Ormad, M.P.; Mosteo, R.; Ovelleiro, J.L. Photocatalytic degradation of pesticides in natural water: Effect of hydrogen peroxide. *Int. J. Photoenergy* **2012**, *2012*, doi:10.1155/2012/371714.
55. Bullock, G.L.; Summerfelt, S.T.; Noble, A.C.; Weber, A.L.; Durant, M.D.; Hankins, J.A. Ozonation of a recirculating rainbow trout culture system I. Effects on bacterial gill disease and heterotrophic bacteria. *Aquaculture* **1997**, *158*, 43–55.

© 2013 by the authors; licensee MDPI, Basel, Switzerland. This article is an open access article distributed under the terms and conditions of the Creative Commons Attribution license (<http://creativecommons.org/licenses/by/3.0/>).